Calibration of a liquid xenon detector with $^{83}Kr^{m}$

L. W. Kastens, S. B. Cahn, A. Manzur, and D. N. McKinsey
Department of Physics, Yale University, Post Office Box 208120, New Haven, CT 06520, USA
(Received 7 June 2009; published 30 October 2009)

We report the preparation of a $^{83}Kr^{m}$ source and its use in calibrating a liquid xenon detector. $^{83}Kr^{m}$ atoms were produced through the decay of ^{83}Rb and introduced into liquid xenon. Decaying $^{83}Kr^{m}$ nuclei were detected through liquid xenon scintillation. Conversion electrons with energies of 9.4 and 32.1 keV from the decay of $^{83}Kr^{m}$ were observed. This calibration source will allow the characterization of the response of noble liquid detectors at low energies. $^{83}Kr^{m}$ may also be useful for measuring fluid flow dynamics, both to understand purification in noble liquid-based particle detectors, as well as for studies of classical and quantum turbulence in superfluid helium.

DOI: 10.1103/PhysRevC.80.045809 PACS number(s): 29.40.Gx, 21.10.Tg, 27.50.+e, 29.40.Mc

I. INTRODUCTION

Much cosmological evidence suggests the existence of dark matter. A favored candidate for dark matter is the WIMP (weakly interacting massive particle), which is the subject of many direct dark matter searches [1–4], in which nuclear elastic scatters present a potential WIMP signal. Detector technologies using liquefied noble gases have recently become an important method of direct searches for WIMPs, with several experiments achieving strong WIMP-nucleon cross-section limits over the past few years [5–8]. Calibration of such detectors at low energies (tens of keV) becomes more difficult as detector sizes are increased owing to the self-shielding capability of large detectors.

The doping of a low-energy radioactive source into the active material of the detector would allow for efficient production of low-energy events in the fiducial volume of large detectors. The calibration of the fiducial volume of the XENON10 detector was effected by the introduction of two activated xenon isotopes produced at Yale University [9] and shipped to Gran Sasso National Laboratory: ^{129m}Xe and ^{131m}Xe, which emit 236- and 164-keV γ rays with half-lives of 8.9 and 11.8 days, respectively. Although these isotopes can be used to fill the detector with a temporary calibration source, the energies are higher than those expected from WIMP signals, and their long half-lives prevent their use for frequent calibration. Another such source is derived from ^{83}Rb, which decays to $^{83}Kr^{m}$ with a half-life of 86.2 days. The $^{83}Kr^{m}$ subsequently decays via emission of 32.1- and 9.4-keV conversion electrons with a half-life of 1.83 h [10] (Fig. 1). Such a source is not expected to introduce any long-lived radioisotopes. $^{83}Kr^{m}$ is an important diagnostic tool for studying the β spectrum of tritium to determine the neutrino mass, most recently proposed for use with KATRIN [11].

The LUX (Large Underground Xenon) experiment, currently in fabrication, will be deployed to the Homestake Mine in South Dakota as a part of the Sanford Underground Science and Engineering Laboratory (SUSEL). LUX is expected to achieve a WIMP sensitivity at least two orders of magnitude better than the recent XENON10 and CDMS-II experiments [5,12]. $^{83}Kr^{m}$ can be used to calibrate the energy scale in the fiducial region, create maps of detector scintillation and ionization response, and monitor detector stability.

II. EXPERIMENTAL APPARATUS

The liquid xenon detector used to test $^{83}Kr^{m}$ calibration is located at Yale University (Fig. 2). The active liquid xenon target is about 5 cm in diameter and 2 cm in height, containing 150 g of liquid xenon surrounded by PTFE (Teflon) for UV scintillation light reflection and viewed by two Hamamatsu R9869 photomultipliers (PMTs). The R9869 PMT has a bialkali photocathode with aluminum strip pattern and a quartz window with a quantum efficiency of 36% for xenon scintillation light at 175 nm. Three stainless steel mesh grids, with 90% optical transparency, and a copper ring are installed for two-phase operation but were not energized in this experiment. The liquid xenon, PMTs, PTFE, and grids are contained in an 11-cm-diameter stainless steel cylinder, located in an aluminum vacuum cryostat and cooled by a pulse-tube refrigerator (Fig. 3). The cryogenic system is described elsewhere [9].

The gains of the two PMTs are measured from the single photoelectron (pe) spectra by using light emitted from an LED inside the liquid xenon detector. The liquid xenon detector is calibrated with 122- and 133-keV γ rays from a ^{57}Co source outside the cryostat. The scintillation signal yield for the ^{57}Co γ rays in liquid xenon is measured to be 11.1 pe/keV (Fig. 4).

The ^{83}Rb source is infused in 2 g of zeolite located in the bottom arm of a VCR cross [13]. The side arms of the cross allow gas to flow through the chamber, and filters prevent the introduction of zeolite into the xenon system. The top arm of the cross allows the zeolite to be primed with ^{83}Rb in 1M HCl solution. Then 700 nCi of ^{83}Rb was loaded into a 10-μl syringe from a 5-ml glass septum vial, discharged from the syringe into the zeolite, sealed in the cross, then baked at 80°C for several days. At each step, the amount of ^{83}Rb was measured by monitoring its combined 521-, 530-, and 553-keV γ-ray emission with a 5-cm cylindrical NaI detector (see Fig. 5).

While the Rb stays attached to the zeolite [14], the $^{83}Kr^{m}$ reaches an equilibrium rate of 16 kBq upon introduction to the detector. The $^{83}Kr^{m}$ was doped into the detector by circulating xenon with a diaphragm pump at 2 l/min through the $^{83}Kr^{m}$ generator for 5 min (Fig. 6). Circulation then bypassed the $^{83}Kr^{m}$ generator, but still passed through the getter.

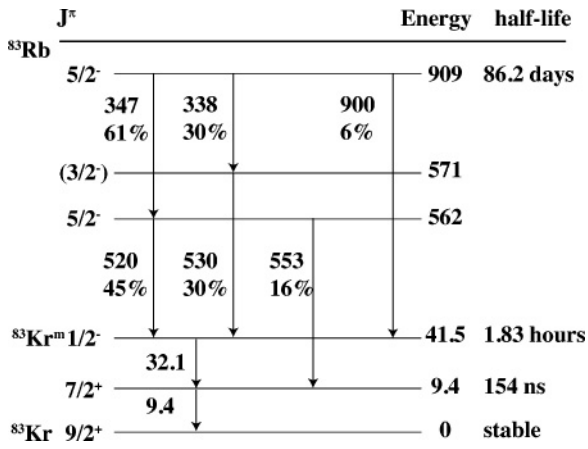

FIG. 1. Energy level diagram (in keV) for the ^{83}Rb decay. Each ^{83}Rb decays 75% of the time to the long-lived isomeric ^{83}Kr^{m} level 41.5 keV above the ground state, which subsequently decays in two steps, emitting a 32.1- and then a 9.4-keV conversion electron.

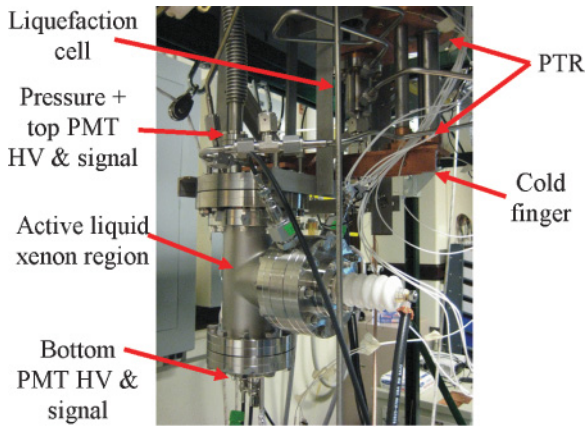

FIG. 2. (Color online) Photograph of apparatus for ^{83}Kr^{m} measurement in liquid xenon.

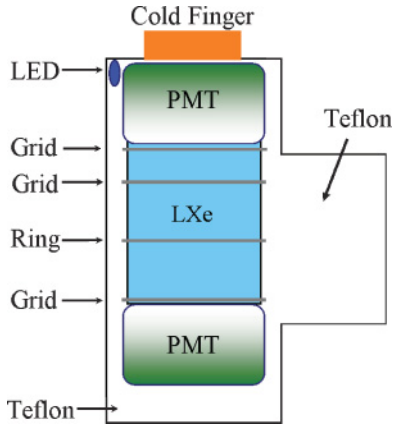

FIG. 3. (Color online) Schematic of apparatus for ^{83}Kr^{m} measurement in liquid xenon.

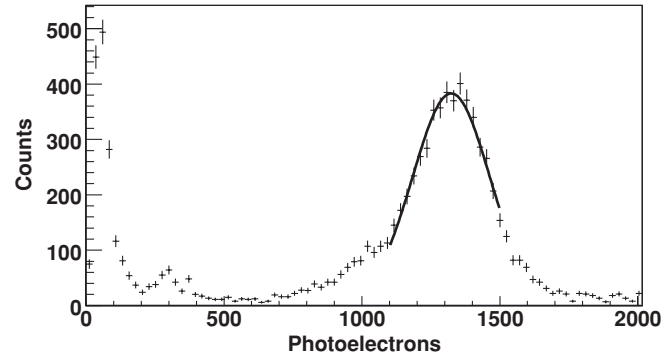

FIG. 4. Calibration peak from ^{57}Co γ rays, indicating a signal yield of 11.1 pe/keV.

III. DATA ANALYSIS AND RESULTS

Events were recorded to computer via a 250-MHz, 12-bit CAEN V1720 waveform digitizer for later analysis. Data acquisition was triggered by coincident PMT pulses, each greater than 1 keV (11 pe). The trigger rate was recorded via a counter and monitored throughout the experiment. After introducing ^{83}Kr^{m} into the xenon flow the trigger rate increased for 30 min, then began to decay with a half-life consistent with 1.83 h after another 60 min.

The digitized PMT waveforms were analyzed to quantify the response of the detector to ^{83}Kr^{m} decays. Each PMT waveform was scanned for a primary and secondary pulse. To find the energy deposited, each pulse was integrated, then divided by the gain of the PMT to determine the number of photoelectrons detected. The number of photoelectrons in each PMT was added and the sum divided by the signal yield determined from the ^{57}Co calibration. The first pulse was the larger primary pulse corresponding to the 32.1-keV conversion electron. The secondary pulse corresponded to the 9.4-keV conversion electron, emitted following the first conversion electron with a 154-ns half-life.

Several cuts were applied to the waveforms. A cut on the asymmetry between the two PMTs was made to optimize the

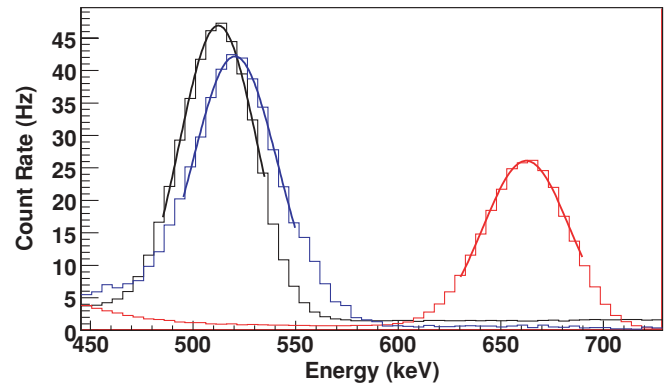

FIG. 5. (Color online) After sealing the ^{83}Kr^{m} generator, a NaI detector confirms the decay of ^{83}Rb within the generator. The black curve is a 511-keV γ-ray peak from ^{22}Na, the red curve is a 662-keV γ-ray peak from ^{137}Cs, and the blue curve is a peak due to 521-, 530-, and 553-keV γ rays from ^{83}Rb decaying in the ^{83}Kr^{m} generator.

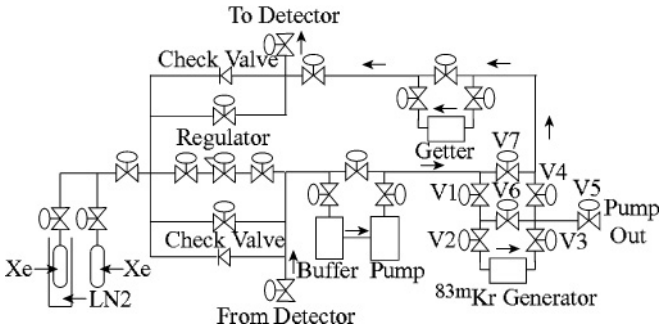

FIG. 6. The gas handling system for the xenon detector. The $^{83}Kr^{m}$ generator is attached to valves V1 and V4 of the main system and may be separately evacuated while the detector is in operation. Closing valve V7 and opening valves V1–V4 permits the $^{83}Kr^{m}$ to be entrained in xenon flow into the detector.

energy resolution. The efficiency of this cut was 50% for primary pulses and 22% for secondary pulses. Primary and secondary pulses that occurred close together in time hurt energy resolution. To mitigate this effect, primary pulses with a corresponding secondary pulse less than 4 keV or greater than 14 keV were cut. Similarly, secondary pulses that had a corresponding primary pulse less than 25 keV and greater than 37 keV were cut. The cut to the primary pulse had a 44% efficiency, whereas the cut to the secondary pulse had a 56% efficiency.

By combining all of the $^{83}Kr^{m}$ data sets taken over the course of several hours, peaks corresponding to the 9.4- and 32.1-keV conversion electrons were fit with a Gaussian function using a least-squares fitting method. We found peaks at energies of 31.550 ± 0.019 and 9.014 ± 0.010 keV with a linear energy scale derived from the ^{57}Co calibration (Fig. 7). Since the scintillation efficiency of liquid xenon may decrease slightly at lower energies [15], these peaks are consistent with the 32.1- and 9.4-keV conversion electrons from $^{83}Kr^{m}$.

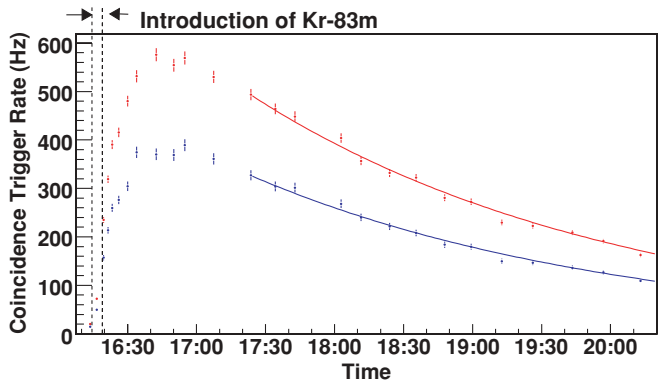

FIG. 7. (Color online) Experimental $^{83}Kr^{m}$ peaks measured with liquid xenon scintillation, corresponding to the 9.4- and 32.1-keV conversion electrons. Noise events create a non-Gaussian tail in the 9.4-keV peak below 5 keV, whereas above 38 keV a non-Gaussian tail is seen for the 32.1-keV peak due to 32.1- and 9.4-keV conversion electrons, which cannot be resolved.

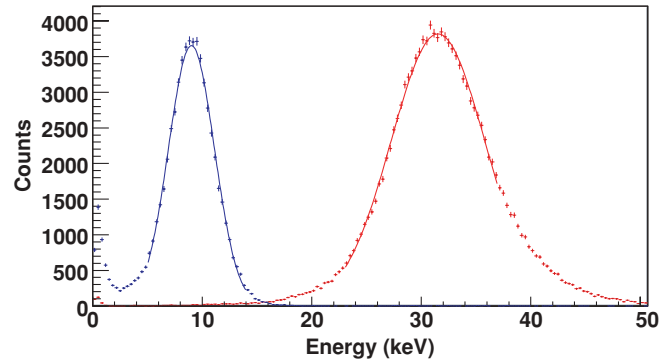

FIG. 8. (Color online) The activities of both energy peaks after doping $^{83}Kr^{m}$ into the liquid xenon detector. An exponential was fit to the coincidence trigger rate after it began to decay subsequent to the introduction of the $^{83}Kr^{m}$. The standard root fitting routine was used. The red curve is the 32.1-keV conversion electron with a measured half-life of 1.856 ± 0.036 h, and the blue curve is the 9.4-keV conversion electron with a measured half-life of 1.846 ± 0.049 h. The decays of both peaks were consistent with the previously measured 1.83-h half-life of $^{83}Kr^{m}$.

The 9.4-keV peak had a 23% resolution (σ/E), whereas the 32.1-keV peak had a 14% resolution.

We then individually fit 26 sets of data taken over four hours. The 9.4- and 32.1-keV peaks were integrated to find the peak count rate as a function of time. The decay time of each peak was found by fitting an exponential to the count rate data. The half-lives were measured to be 1.856 ± 0.036 h for the 32.1-keV conversion electron and 1.846 ± 0.049 h for the 9.4-keV conversion electron, both consistent with the reported 1.83-h half-life of $^{83}Kr^{m}$ (Fig. 8). The time between the primary and secondary pulses was fit to an exponential. We found the half-life of $^{83}Kr^{\frac{7}{2}^{+}}$ to be 156.94 ± 0.34 ns, consistent with the previously measured 154.4 ± 1.1 ns (Fig. 9) [16].

IV. DISCUSSION

Based on the experiment just described, $^{83}Kr^{m}$ may be introduced into low-background liquid xenon detectors to characterize the scintillation and ionization response at

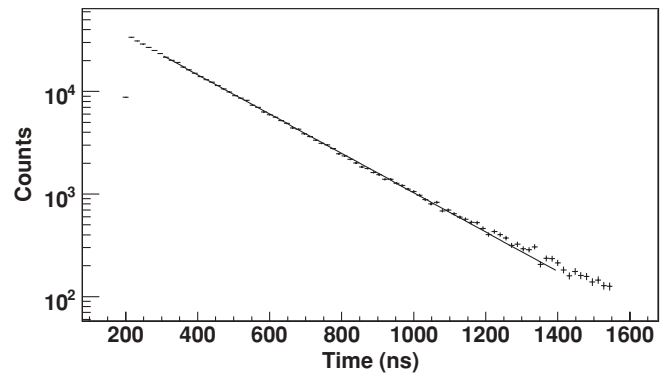

FIG. 9. The half-life of $^{83}Kr^{\frac{7}{2}^{+}}$ was measured to be 156.94 ± 0.32 ns, in agreement with previous measurements.

energies similar to those expected from WIMP-nucleon scatters. Typically the newly purified liquid xenon is continuously introduced into the detector, and less pure xenon is removed to a room-temperature purification system. With such a detector running in a low-background mode, the xenon gas flow may be diverted through a section of plumbing containing ^{83}Rb-infused zeolite. The xenon flow will entrain ^{83}Kr^{m} atoms, pass through a getter to remove impurities, be liquefied, and enter the detector. With sufficient mixing during their 1.83-h half-life, the ^{83}Kr^{m} atoms will spread throughout the active detector volume, allowing all parts of the detector to be calibrated for scintillation and ionization response. It is not necessary for the ^{83}Kr^{m} atoms to spread *evenly* through the detector to measure the scintillation and ionization response, though an even spread of ^{83}Kr^{m} activity would allow a calibration of the fiducial mass.

A pulsed flow of ^{83}Kr^{m} atoms would allow the mixing of liquid xenon to be visualized in time, as the imaging of individual ^{83}Kr^{m} decays will indicate the velocity flow of newly introduced liquid xenon. The mixing of the liquid xenon flow is of interest for liquid xenon detector operation as the degree of mixing is important for quantifying the effectiveness of purification. With a high degree of mixing, the purity may be improved by $1/e$ at best per volume exchange, but if there is little mixing, the degree of purification is limited by the efficiency of the purification method.

Noble liquid detectors using liquid argon, liquid neon, and liquid helium might also be calibrated with ^{83}Kr^{m}, though some fraction of the ^{83}Kr^{m} atoms will freeze out on detector surfaces. Kr dissolves in liquid argon, but in liquid neon and liquid helium, Kr atoms would eventually freeze out. In appropriate conditions, the time scale for Kr freeze-out might be many times the ^{83}Kr^{m} half-life.

The seeding of ^{83}Kr^{m} might also be used in the visualization of fluid flow in cryogenic helium. In liquid helium, a decaying ^{83}Kr^{m} atom will produce a localized population of approximately 2000 helium triplet molecules, which may then be imaged using laser-induced fluorescence [17]. At sufficiently low temperatures, ^{83}Kr^{m} atoms will be trapped by quantized vortices in superfluid helium, and so the imaging of ^{83}Kr^{m} decays through laser-induced fluorescence may permit the monitoring of vortex dynamics and quantum turbulence decay [18]. Likewise, introduction of ^{83}Kr^{m} atoms into a well-defined point in a helium flow at higher temperature should allow the visualization of classical turbulence in liquid or gaseous helium [19].

The experiment described here will be augmented with additional experiments in which this liquid xenon detector is operated in two-phase mode (where ionization is drifted through the liquid xenon and detected via proportional scintillation). This mode of operation will allow the electron drift length to be measured following the introduction of ^{83}Kr^{m} into the detector to verify that the liquid xenon purity is not adversely affected by outgassing of the zeolite.

ACKNOWLEDGMENTS

The authors would like to recognize the assistance of Jeff Ashenfelter and Kevin Charbonneau in the acquisition of the ^{83}Rb and preparation of the ^{83}Rb-infused zeolite. The authors would also like to thank Joseph Formaggio, who pointed them to the papers of Venos *et al.* describing the preparation of ^{83}Rb-infused zeolite for the calibration of KATRIN. This work was supported by NSF Grant No. PHY-0800526.

[1] M. W. Goodman and E. Witten, Phys. Rev. D **31**, 3059 (1985).
[2] G. Jungman, M. Kamionkowski, and K. Griest, Phys. Rep. **267**, 195 (1996).
[3] G. Bertone, D. Hooper, and J. Silk, Phys. Rep. **405**, 279 (2005).
[4] R. J. Gaitskell, Annu. Rev. Nucl. Part. Sci. **54**, 315 (2004).
[5] J. Angle *et al.*, Phys. Rev. Lett. **100**, 021303 (2008).
[6] G. J. Alner *et al.*, Astropart. Phys. **23**, 444 (2007).
[7] V. N. Lebedenko *et al.*, Phys. Rev. D **80**, 052010 (2009).
[8] R. Brunetti *et al.*, New Astron. Rev. **49**, 265 (2005).
[9] K. Ni *et al.*, Nucl. Instrum. Methods A **582**, 569 (2007).
[10] D. Venos *et al.*, Appl. Radiat. Isotopes **63**, 323 (2005); D. Venos *et al.*, Nucl. Instrum. Methods A **560**, 352 (2006); S.-C. Wu, Nucl. Data Sheets **92**, 893 (2001).
[11] KATRIN Collaboration, arXiv:hep-ex/0109033v1.
[12] D. Akerib *et al.*, Phys. Rev. Lett. **102**, 011301 (2009).
[13] Supelco molecular sieve 5A (Activated) 8/12 mesh, Lot:1638-82.
[14] This was checked by administering 10^{10} more ^{nat}Rb (in aqueous RbCl solution) to a sample of zeolite and measuring the Rb escaping into the vacuum with a residual gas analyzer while pumping. There was no Rb above baseline, indicating a suppression of better than 10^{10}.
[15] M. Yamashita *et al.*, Nucl. Instrum. Methods A **535**, 692 (2004).
[16] S. C. Wu, Nucl. Data Sheets **92**, 893 (2001).
[17] D. N. McKinsey, W. H. Lippincott, J. A. Nikkel, and W. G. Rellergert, Phys. Rev. Lett. **95**, 111101 (2005); W. G. Rellergert, S. B. Cahn, A. Garvan, J. C. Hanson, W. H. Lippincott, J. A. Nikkel, and D. N. McKinsey, *ibid.* **100**, 025301 (2008); W. Guo *et al.*, arXiv:0904.0732v2.
[18] W. F. Vinen, J. Low Temp. Phys. **145**, 7 (2006).
[19] J. J. Niemela and K. R. Sreenivasan, J. Low Temp. Phys. **143**, 163 (2006).